Supplemental Figure 1

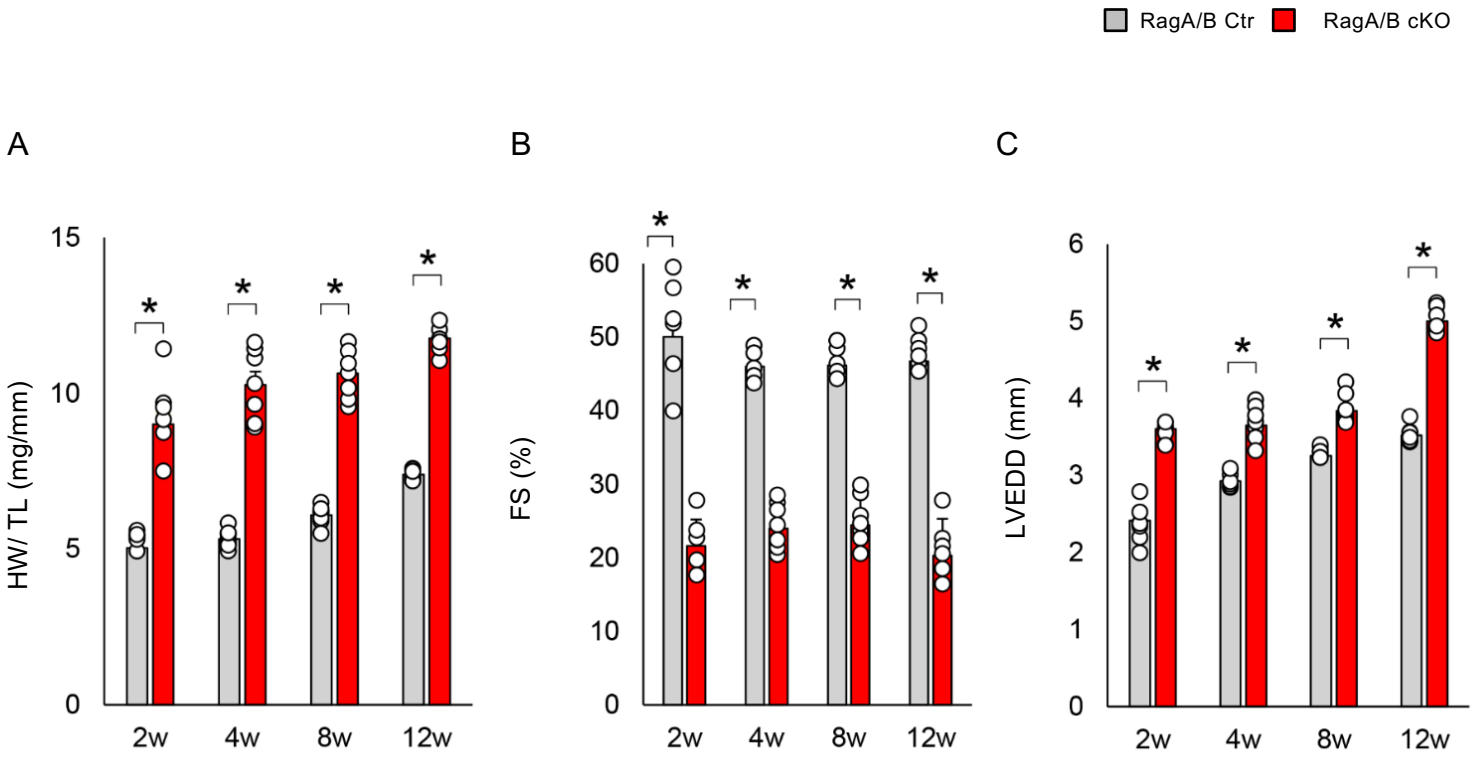

Supplemental Figure 1 Time course of cardiac morphology and left ventricular function in *RagA/B* cKO mice. **(A)** Quantitative analysis of total heart weight to tibia length ratio (HW/TL) at 2, 4, 8 and 12 weeks. n =6-7. **(B, C)** Quantitative analyses of echocardiographically evaluated FS and LVEDD at 2, 4, 8 and 12 weeks. n =6. Results are expressed as mean ± SEM. *p<0.05 by ANOVA.

Supplemental Figure 2

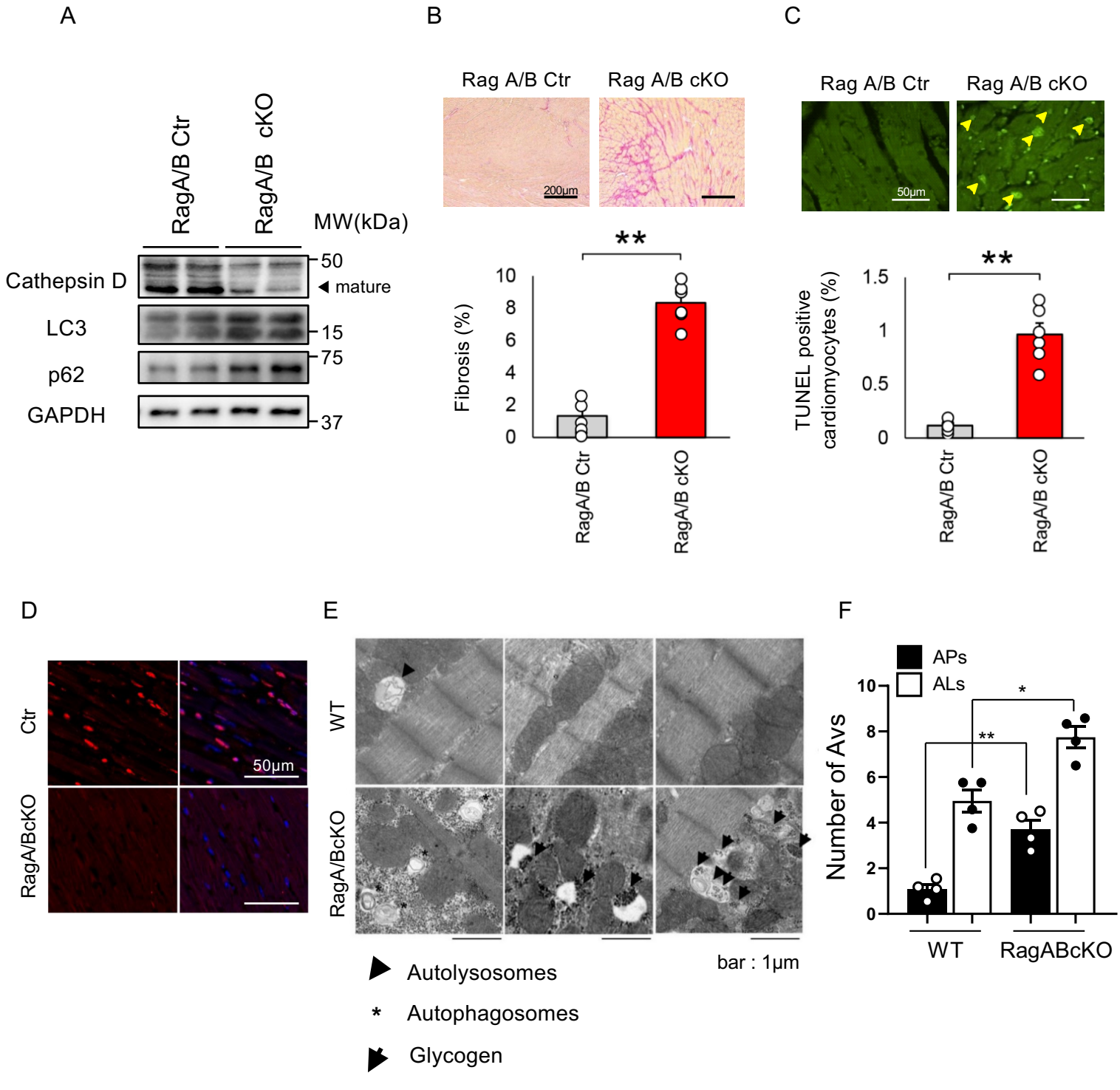

Supplemental Figure 2 *RagA/B* cKO mice exhibit decreases in the mature form of cathepsin D, severe cardiac fibrosis and death of CMs reminiscent of LSD.
(A) Representative immunoblots of Ctr and *RagA/B* cKO mouse heart homogenates. Blots run in parallel, contemporaneously, using identical samples are shown. **(B)** Representative micrographs of picrosirius red staining and quantitative analysis of interstitial fibrosis in Ctr and *RagA/B* cKO mouse hearts. n=6. **(C)** Representative micrographs of TUNEL staining and quantitative analyses in Ctr and *RagA/B* cKO mouse hearts. n=6. **(D)** Representative images of HMGB1 in *RagA/B* Ctr and cKO mouse hearts at 12 weeks old. **(E)** Representative images of electron microscopic analyses of myocardial sections from wild type (WT) and *RagA/B* cKO mice. Results are representative of 4 experiments. **(F)** Autophagy vacuoles (AVs), including Autophagosomes (APs) and autolysosomes (ALs), were counted. n=4. Values were measured from more than 10 different areas per mouse. Results are expressed as mean ± SEM. *$p<0.05$, **$p<0.01$ by ANOVA.

Supplemental Figure 3

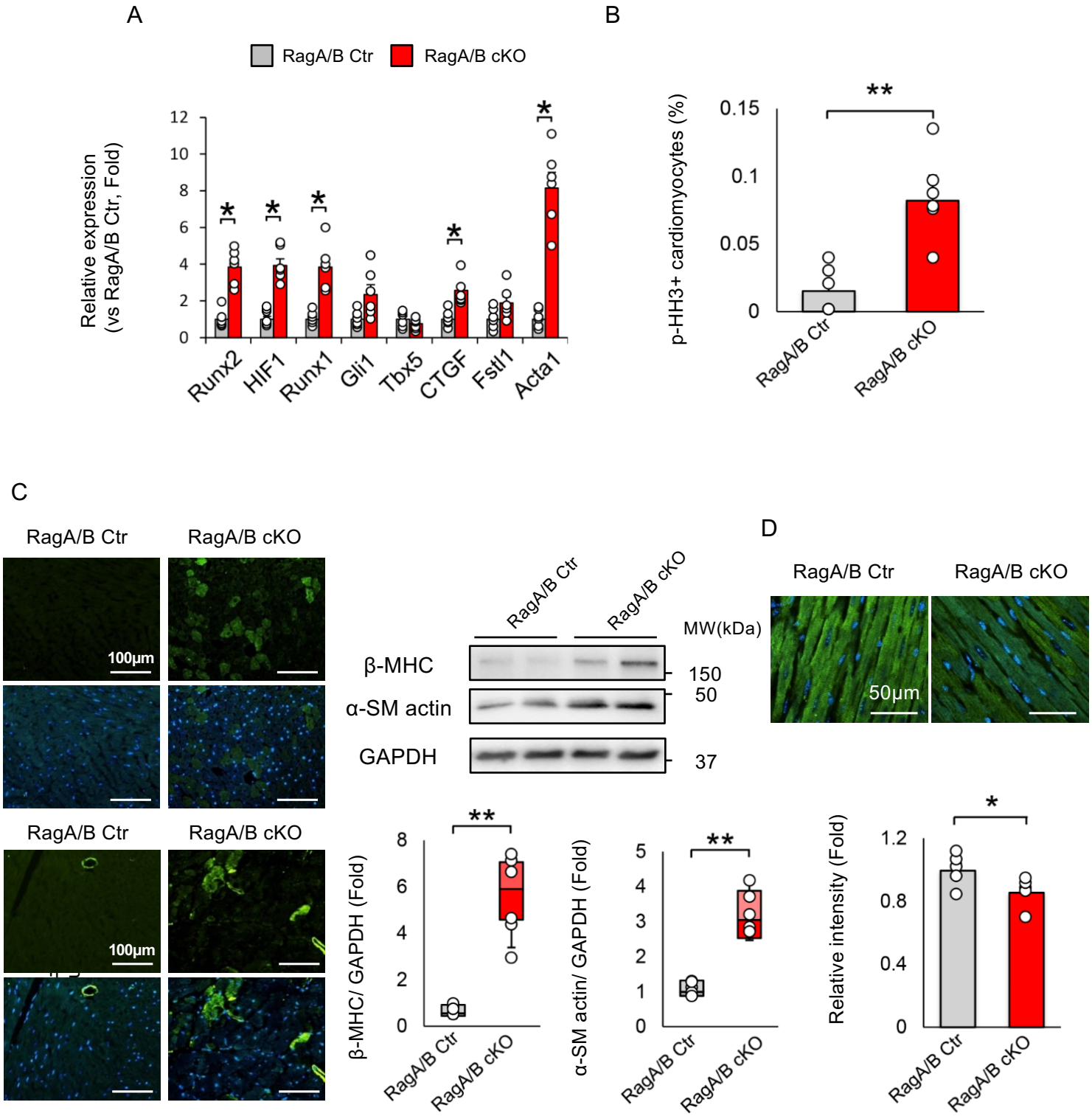

Supplemental Figure 3 The characteristics of *RagA/B* cKO mouse hearts.
(A) Relative mRNA expression of known YAP target genes in Ctr and *RagA/B* cKO mouse hearts. n=6. **(B)** Quantitative analyses of pHH3 positive CMs in Ctr and *RagA/B* cKO mouse hearts at 12 weeks. n=6. **(C)** Representative micrographs and quantitative analyses of MYH7 and ACTA2 immunostaining. Co-staining with DAPI was conducted. n=6. Representative images and quantitative analyses of MYH7/GAPDH and ACTA2/GAPDH in Ctr and *RagA/B* cKO mouse hearts. Blots run in parallel, contemporaneously, using identical samples are shown. n=6. **(D)** Representative micrographs and quantitative analyses of cTnT immunostaining. Co-staining with DAPI was conducted. n =5. Results are expressed as mean ± SEM in A, B and D. In C, results are shown as box plots, showing the median (center line) and interquartile range (IQR). Whiskers represent minima and maxima within 1.5 IQR as indicated. *p<0.05, **p<0.01 by ANOVA.

Supplemental Figure 4

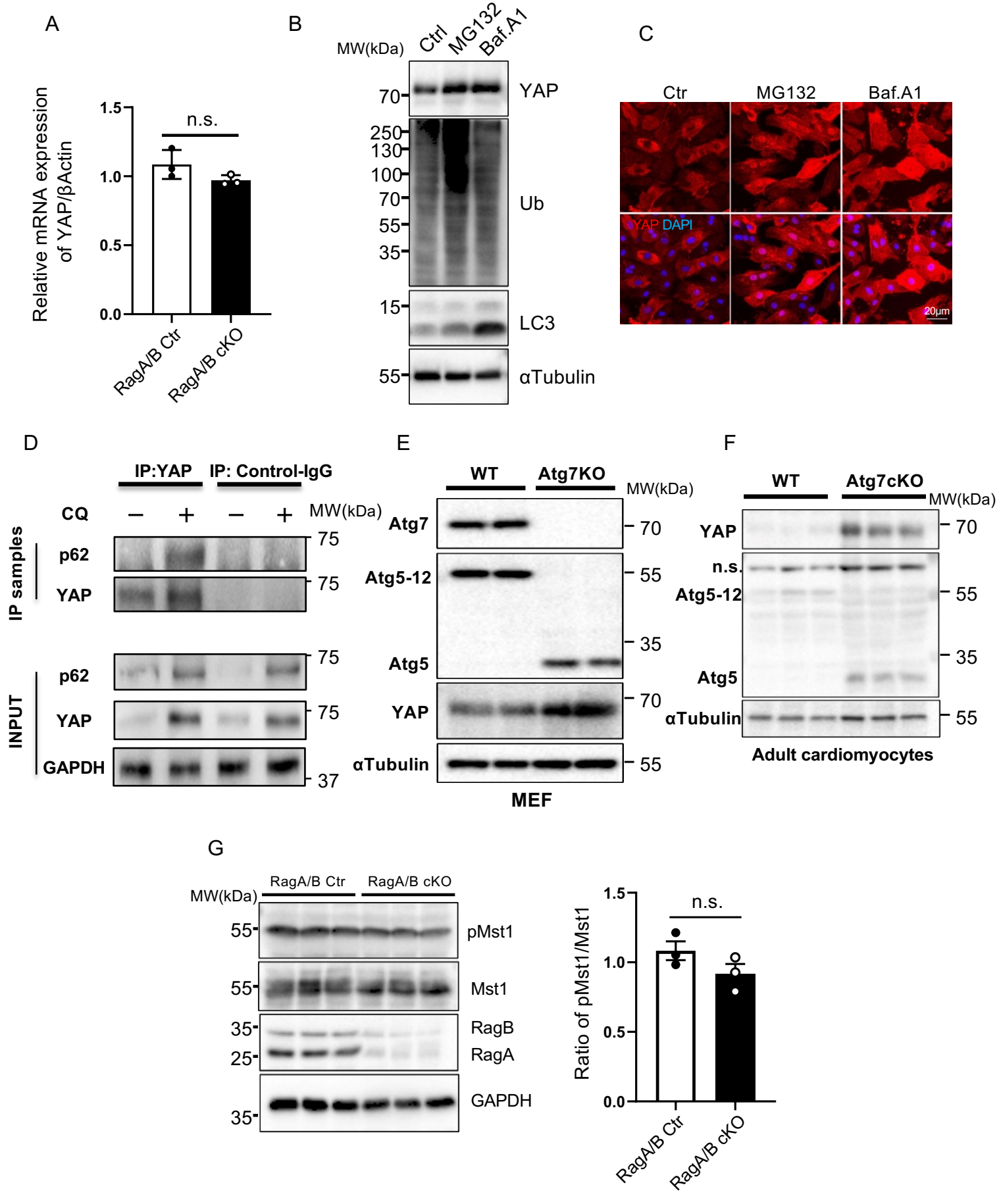

Supplemental Figure 4 YAP interacts with p62.
(A) Relative mRNA expression of YAP in Ctr and *RagA/B* cKO mouse hearts. n=3. **(B, C)** Neonatal CMs were transduced with adenovirus harboring YAP for 24 hours and treated with DMSO, 10 μM MG132 or 20 nM Bafilomycin A1 for an additional 24 hours. In B, representative images of immunoblots are shown. In C, representative images of YAP and DAPI in cultured CMs *in vitro* are shown. In B and C, n=3. **(D)** Neonatal CMs were transduced with adenovirus harboring sh-Ctr or sh-*RagA/B* and then treated with or without chloroquine (CQ). CM lysates were subjected to immunoprecipitation (IP) with anti-YAP antibody. The original lysates (input) and the IP samples were then subjected to immunoblot analyses. Representative images are shown. For inputs, a blot run in parallel, contemporaneously, using identical samples is shown. n=3. **(E)** Wild type (WT) and *Atg7* knockout MEF cell lysates were subjected to immunoblot analyses. **(F)** Adult CMs were isolated from WT and *Atg7* cKO mouse hearts and cell lysates were prepared. In E and F, cell lysates were subjected to immunoblot analysis using anti-Atg7, anti-Atg5, anti-YAP and anti-αTubulin antibodies. (n=2 (MEF) and n=3 (isolated adult CMs)) **(G)** Representative immunoblots of Ctr and *RagA/B* cKO mouse heart homogenates. Blots run in parallel, contemporaneously, using identical samples are shown. Quantitative analyses of pMst1/Mst1 are shown. n =3. Results are expressed as mean ± SEM. n.s., not significant.

Supplemental Figure 5

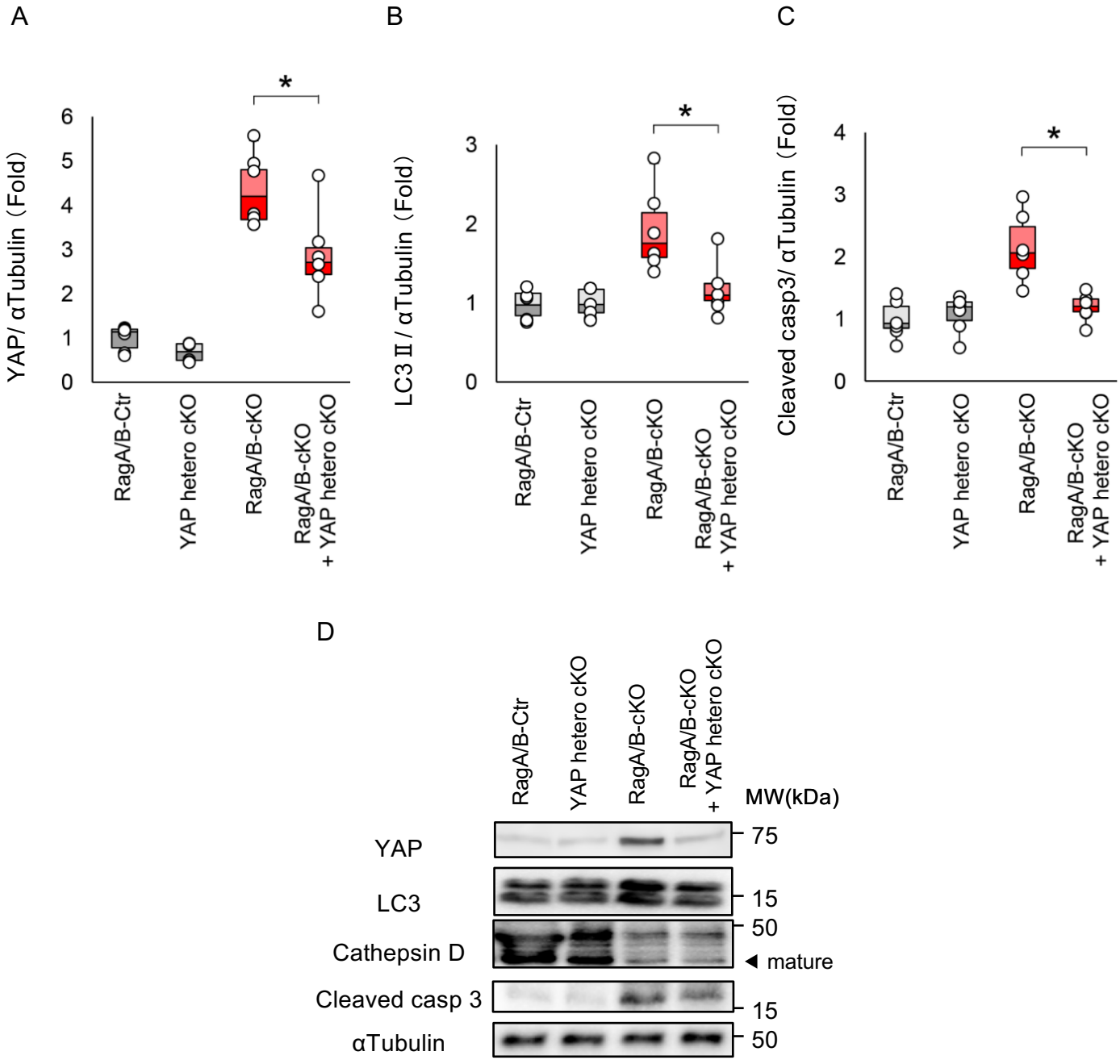

Supplemental Figure 5 The effects of heterozygous deletion of YAP in *RagA/B* cKO mouse hearts.
Quantitative analyses of immunoblots for YAP/αTubulin **(A)**, LC3 Ⅱ /αTubulin **(B)** and Cleaved caspase3/αTubulin **(C)** in mouse hearts. n=6. Analyses were carried out at 12 weeks of age. **(D)** Representative immunoblots of heart homogenates, demonstrating the reproducibility of the results shown in Figure 3F. Blots run in parallel, contemporaneously, using identical samples are shown. Results are shown as box plots, showing the median (center line) and interquartile range (IQR). Whiskers represent minima and maxima within 1.5 IQR as indicated. *p<0.05 by ANOVA.

Supplemental Figure 6

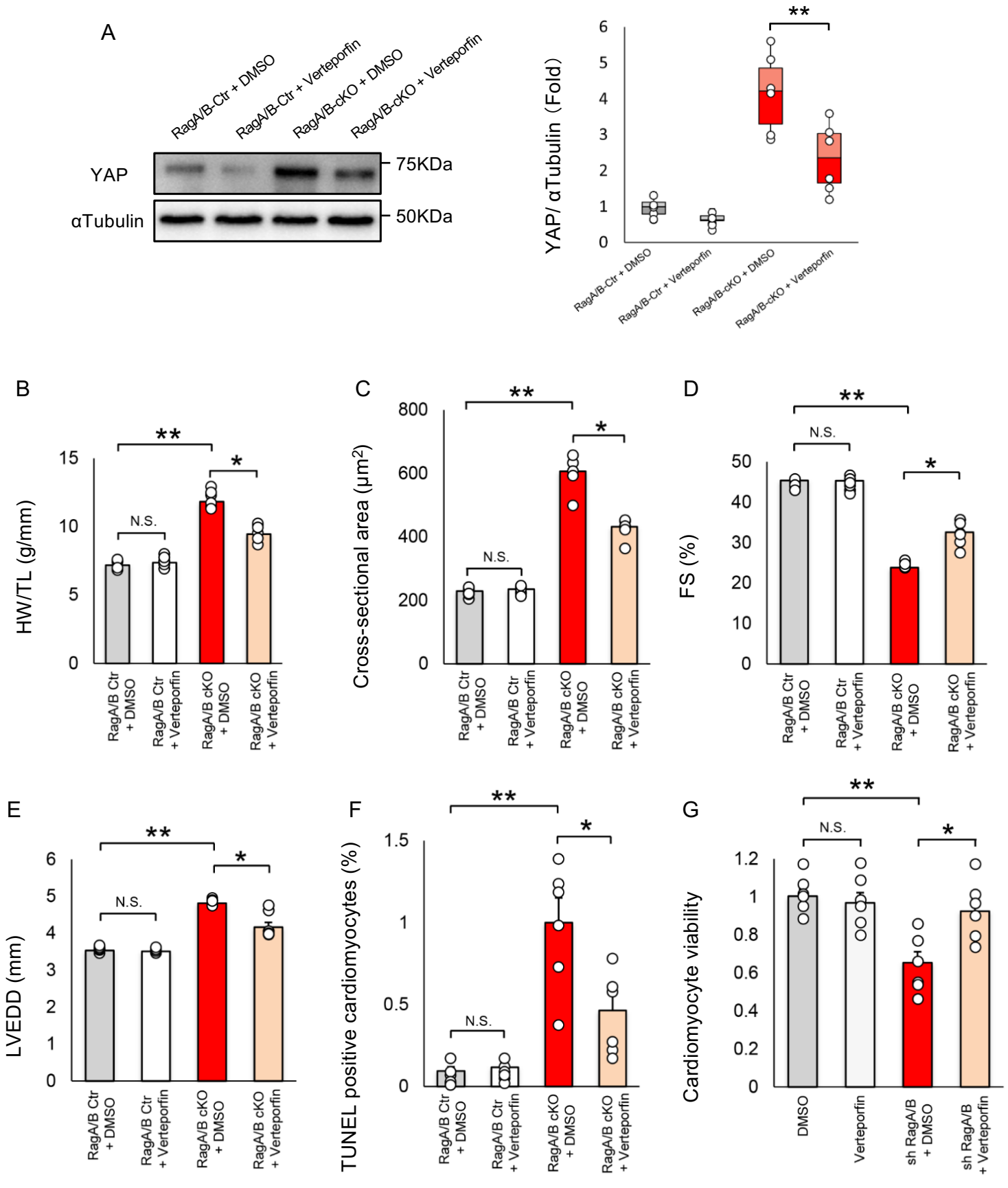

Supplemental Figure 6 Pharmacological inhibition of YAP by verteporfin suppresses cardiac hypertrophy and heart failure in *RagA/B* cKO mice.

(A) The effects of verteporfin upon YAP in control and *RagA/B* cKO mouse hearts. Analysis was carried out at 12 weeks of age. Quantitative analyses of immunoblots for YAP/αTubulin are shown. n=6.**(B)** Quantitative analyses of heart weight/tibial length (HW/TL). n=6. **(C)** Quantitative analysis of cross-sectional area. n=6. **(D, E)** Quantitative analyses of echocardiographically evaluated FS and LVEDD. n=6. **(F)** Quantitative analysis of TUNEL positive CMs. In A-F, n=6. **(G)** Cultured CMs were treated with or without Ad-sh-*YAP* in the presence or absence of verteporfin. Cell viability assays were performed with trypan blue dye. n=6. In each preparation, measurement was conducted 2-3 times. In A, results are shown as box plots, showing the median (center line) and interquartile range (IQR). Whiskers represent minima and maxima within 1.5 IQR as indicated. In B-G, results are expressed as mean ± SEM. *$p<0.05$, **$p<0.01$ by ANOVA. N.S.; not significant.

Supplemental Figure 7

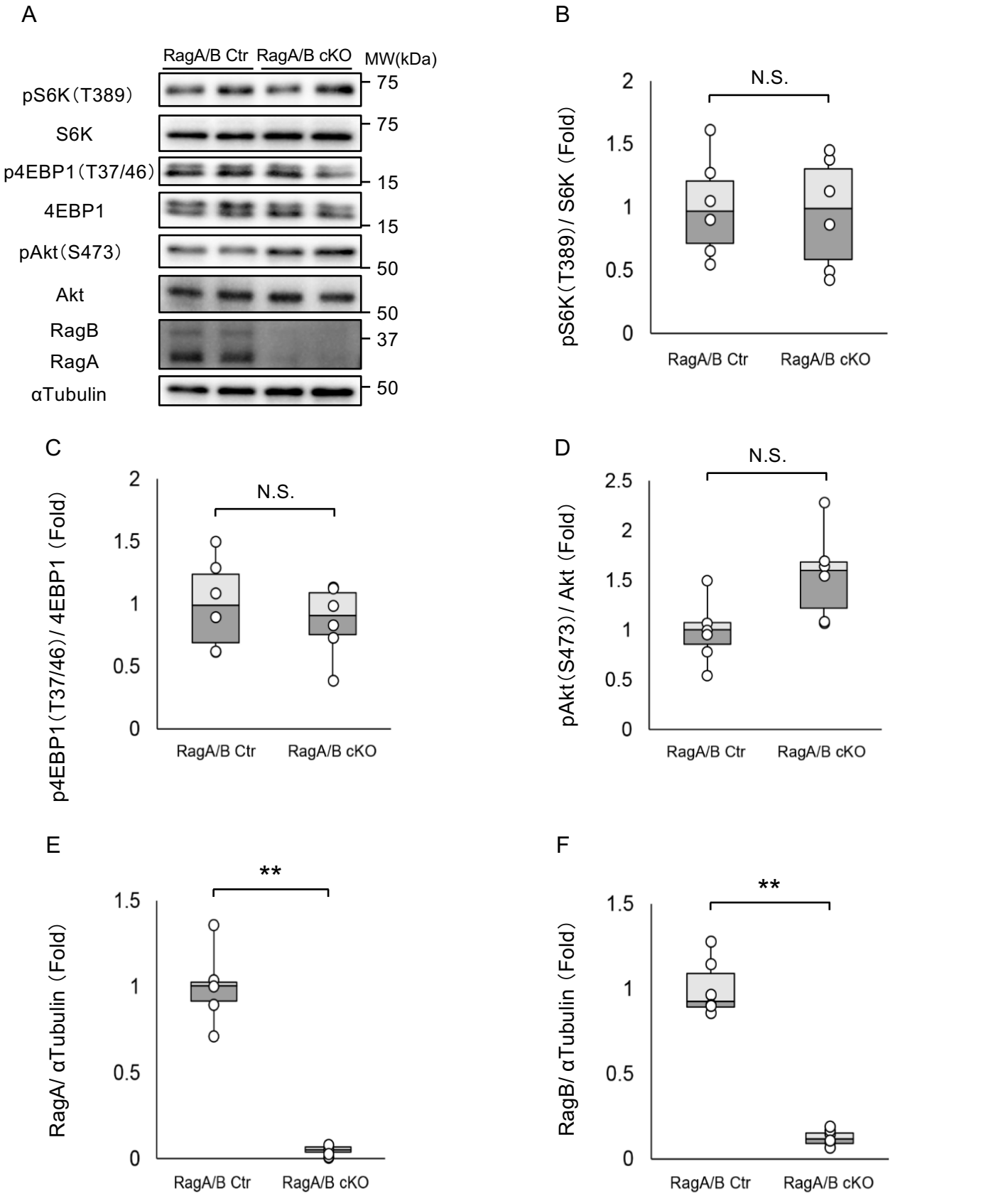

Supplemental Figure 7 The activities of mTORC1 in *RagA/B* cKO mouse hearts.
(A) Representative immunoblots of heart homogenates. Blots run in parallel, contemporaneously, using identical samples are shown. Quantitative analysis of immunoblotting for phospho-S6K/S6K **(B)**, phospho-4EBP1/4EBP1 **(C)** and phospho-Akt(S473) /Akt **(D)** in mouse hearts. n=6. **(E, F)** Quantitative analysis of immunoblotting for RagA/αTubulin **(E)** and RagB/αTubulin **(F)** in mouse hearts. n=5-6. Analyses were carried out at 12 weeks of age. Results are shown as box plots, showing the median (center line) and interquartile range (IQR). Whiskers represent minima and maxima within 1.5 IQR as indicated. *$p<0.05$, **$p<0.01$ by ANOVA. N.S.; not significant.

Supplemental Figure 8

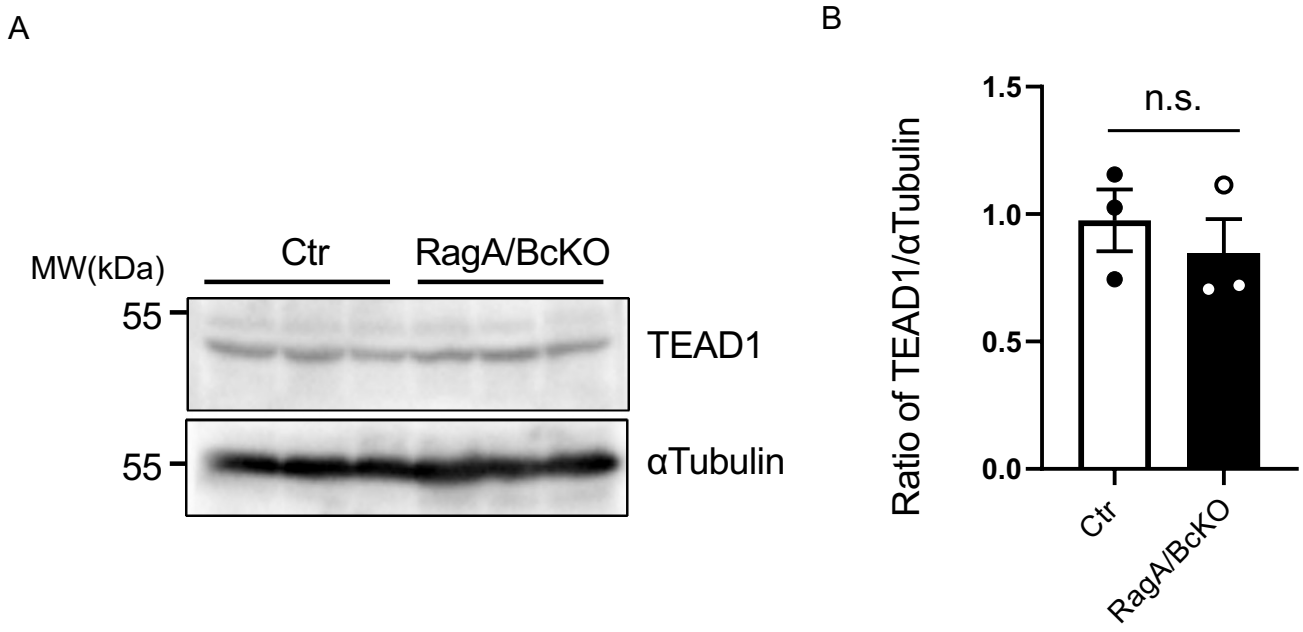

Supplemental Figure 8 The activity of TEAD1 in *RagA/B* cKO mouse hearts.
(A, B) Representative immunoblots of Ctr and *RagA/B* cKO mouse heart homogenates. Quantitative analyses of TEAD1/αTubulin are shown (n =3). Results are expressed as mean ± SEM. n.s., not significant by unpaired t test.

Supplemental Figure 9

A

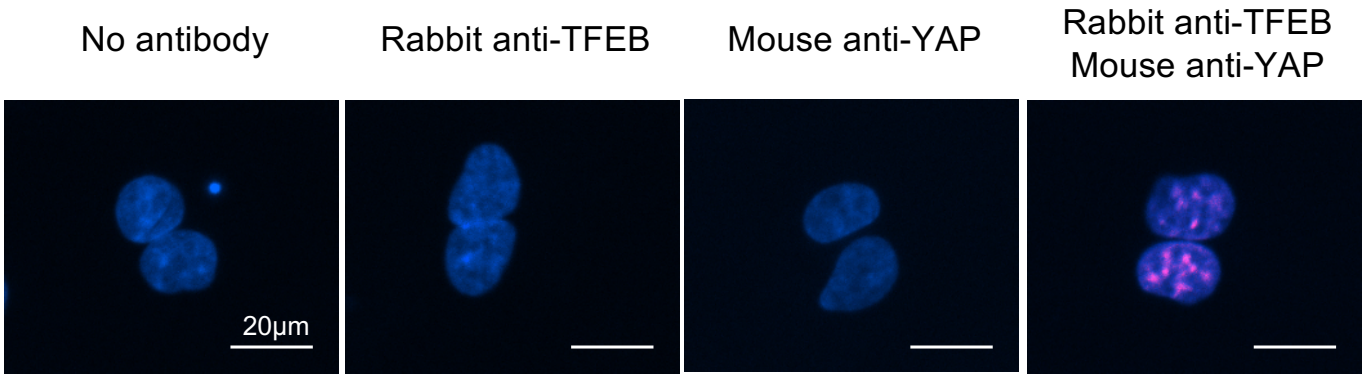

B

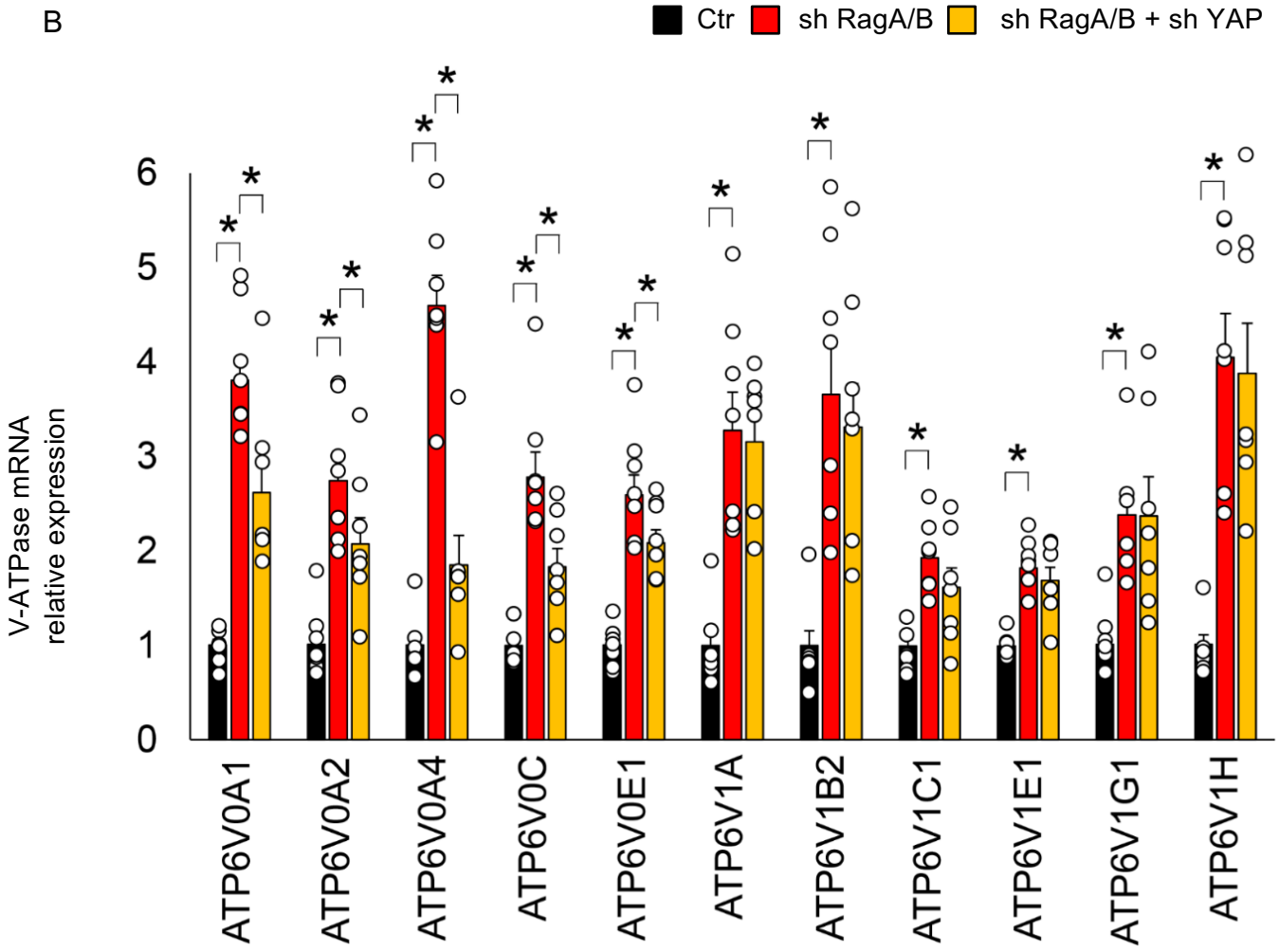

Supplemental Figure 9 YAP physically interacts with TFEB in the nucleus in CMs transduced with Ad-sh-*RagA/B*.

(A) Neonatal CMs were transduced with adenoviruses harboring Ad-sh-*RagA/B*. Proximity Ligation Assays were conducted with anti-YAP and anti-TFEB antibodies. DAPI staining was conducted to mark the nucleus. Staining with no antibody, anti-TFEB antibody, or anti-YAP antibody and double PLA staining with anti-YAP and anti-TFEB staining are shown. n=3.

(B) Relative mRNA expression of V-ATPase subunits, transcriptional targets of TFEB, in Ctr and *RagA/B* cKO mouse hearts. n=5-7. Results are expressed as mean ± SEM. *$p<0.05$ by ANOVA.

Supplemental Figure 10

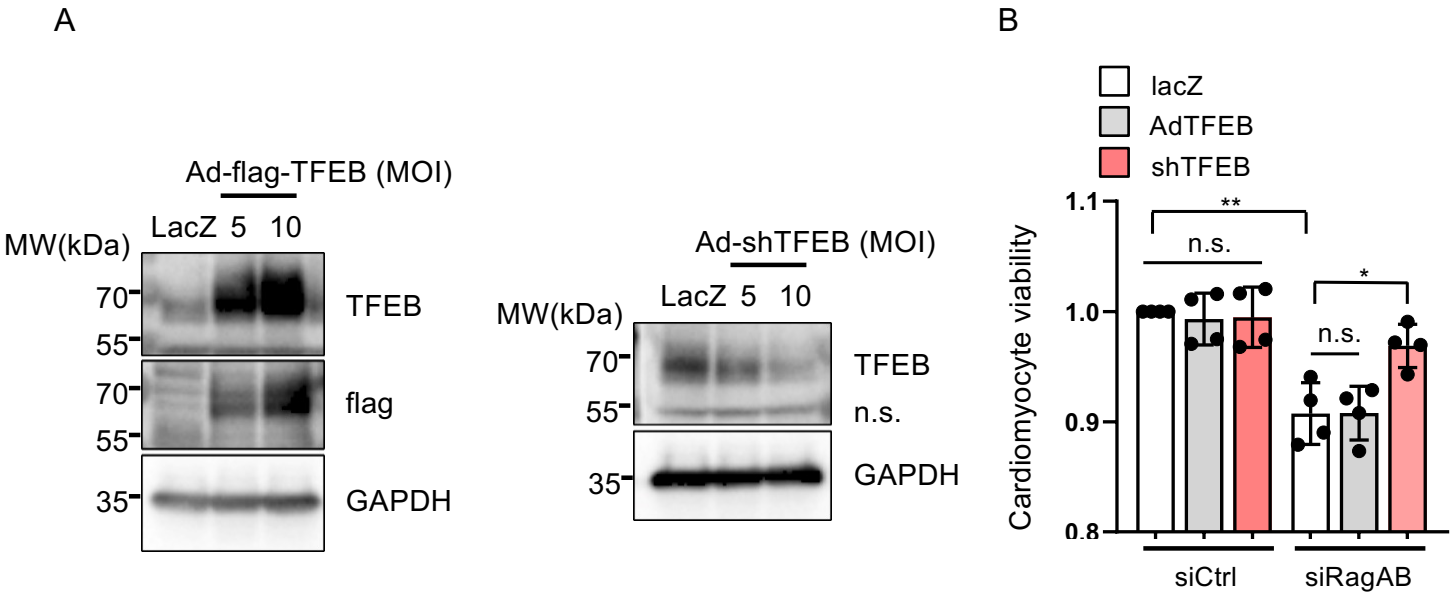

Supplemental Figure 10 The role of TFEB in *RagA/B* cKO mouse hearts.
(A) Neonatal CMs were treated with LacZ, Ad-flag-Tfeb or Ad-shTfeb for 48 hours. Expression levels of Tfeb were evaluated with immunoblotting. **(B)** CMs were treated with siRagA/B, AdTfeb or Ad-shTfeb. After sixty hours, cell viability was quantified by CellTiter-Blue® assays. Results are expressed as mean ± SEM. n=4. Values were measured from more than 8 different wells per experiment.

Supplemental Table

	Control patient (n=8)	Fabry patient (n=7)	*P* value
Age (years)	**54.9 ± 11.4**	**54.6 ± 14.8**	**0.97**
Male sex, n (%)	**2 (25.0)**	**2 (28.6)**	**0.89**
Body mass index (kg/m^2)	**22.4 ± 3.18**	**22.1 ± 3.53**	**0.88**
Echocardiography data			
LVEF (%)	**45.3 ± 4.58**	**69.9 ± 8.29**	**<0.001**
LVFS (%)	**25.9 ± 4.14**	**39.7 ± 5.90**	**<0.001**
IVSTd (mm)	**9.38 ± 0.99**	**13.6 ± 4.24**	**0.03**
PWTd (mm)	**8.75 ± 0.97**	**12.7 ± 4.71**	**0.05**
LVDd (mm)	**52.0 ± 3.16**	**43.6 ± 4.34**	**<0.001**
LVDs (mm)	**38.5 ± 3.54**	**26.6 ± 5.01**	**<0.001**

Supplemental Table. The characteristic of patients with control and Fabry disease

Myocardial biopsy specimens were obtained from patients in Tohoku University Hospital. Control specimens were obtained from patients without Fabry disease, such as dilated cardiomyopathy or ischemic cardiomyopathy, who were matched with age, gender and body mass index. All continuous variables are reported as mean±SD. To compare the two quantitative variables, Welch's t-test was performed.

LVEF; left ventricular Ejection Fraction, LVFS; Left Ventricular Fractional Shortening, IVSTd; interventricular septal thickness, PWTd; posterior wall thickness, LVDd; left ventricular end-diastolic diameter, LVDs; left ventricular end-systolic diameter.